AD-A034 382   PANAMETRICS INC   WALTHAM MASS   F/G 22/2

DESIGN OF INSTRUMENTATION SUITABLE FOR THE INVESTIGATION OF CHA--ETC(U)

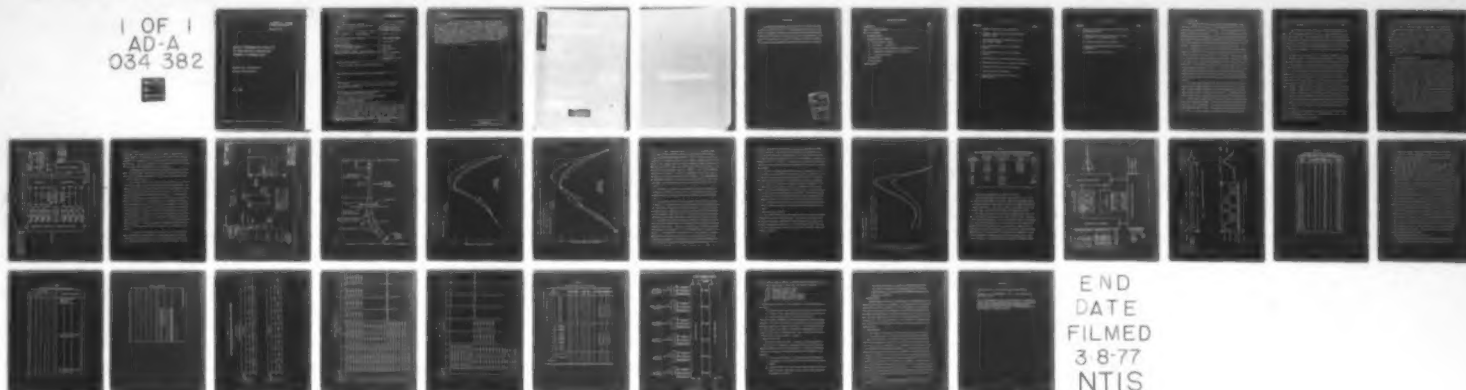JUL 76   J L HUNERWADEL, P R MOREL, F A HANSER   F19628-74-C-0217

UNCLASSIFIED   SCIENTIFIC-2   AFGL-TR-76-0263   NL

1 OF 1
AD-A
034 382

END
DATE
FILMED
3-8-77
NTIS

AD-A034 382

DESIGN OF INSTRUMENTATION SUITABLE FOR THE INVESTIGATION OF CHARGE BUILDUP PHENOMENA AT SYNCHRONOUS ORBIT

PANAMETRICS, INCORPORATED
WALTHAM, MASSACHUSETTS

JULY 1976

REPORT DOCUMENTATION PAGE		READ INSTRUCTIONS BEFORE COMPLETING FORM
1. REPORT NUMBER AFGL-TR-76-0263	2. GOVT ACCESSION NO.	3. RECIPIENT'S CATALOG NUMBER
4. TITLE (and Subtitle) Design of Instrumentation Suitable for the Investigation of Charge Buildup Phenomena at Synchronous Orbit		5. TYPE OF REPORT & PERIOD COVERED Scientific Report - Interim
		6. PERFORMING ORG. REPORT NUMBER Scientific Report #2
7. AUTHOR(s) Jean L. Hunerwadel Frederick A. Hanser Paul R. Morel Bach Sellers		8. CONTRACT OR GRANT NUMBER(s) F19628-74-C-0217
9. PERFORMING ORGANIZATION NAME AND ADDRESS Panametrics, Inc. 221 Crescent St. Waltham MA 02154		10. PROGRAM ELEMENT, PROJECT, TASK AREA & WORK UNIT NUMBERS 1L1R-4E-AA
11. CONTROLLING OFFICE NAME AND ADDRESS Air Force Geophysics Laboratory Hanscom AFB, MA 01731 Contract Monitor: Paul L. Rothwell PHG		12. REPORT DATE July 1976
		13. NUMBER OF PAGES 35
14. MONITORING AGENCY NAME & ADDRESS(if different from Controlling Office)		15. SECURITY CLASS. (of this report) Unclassified
		15a. DECLASSIFICATION/DOWNGRADING SCHEDULE

16. DISTRIBUTION STATEMENT (of this Report)

Approved for public release; distribution unlimited.

17. DISTRIBUTION STATEMENT (of the abstract entered in Block 20, if different from Report)

(Same)

18. SUPPLEMENTARY NOTES

19. KEY WORDS (Continue on reverse side if necessary and identify by block number)

Charge buildup measurement of satellites

Electrostatic analyzers and solid state spectrometers

High time resolution spectrum analysis

Electron and proton detectors

20. ABSTRACT (Continue on reverse side if necessary and identify by block number)

A satellite-borne instrument has been designed to measure the charge buildup phenomena at synchronous orbit. Simultaneous measurements along two orthogonal axes are made. Each axis incorporates 4 electrostatic analyzers (ESA) and 2 solid state spectrometers (SSS). Four ESA's (low energy p, low energy e, high energy p, high energy e) and two SSS's (proton, electron) with four and five energy bins, respectively, in each analyzer provide a logical compromise of energy resolution and high time resolution. The low energy ESA's cover the

DD FORM 1473   EDITION OF 1 NOV 65 IS OBSOLETE

20. Abstract (cont'd)

energy range 0.05 to 1.7 keV; the high energy ESA's cover the 1.7 to 60 keV range. The electron SSS's cover the 30 to 10,000 keV range and the proton SSS's cover the 70 to 35,000 keV range. A complete energy spectrum is generated every 1 second. Design developments on the ESA, SSS, broad band data output and command input circuit are presented. Laboratory tests of an ESA prototype for relative efficiency, response to UV radiation and sensitivity to electrons penetrating the Spiraltron glass walls are discussed. Improved spectral information of the electron SSS is shown in tabular form. The broad-band data output has been expanded to multiplex 64 input signals. A serial entry command input circuit has been incorporated to accommodate the spacecraft integrator's requirements.

FOREWORD

The design development reported herein was carried out under Contract No. F19628-74-C-0217. Special appreciation is given to the Air Force Geophysics Laboratory personnel whose cooperation helped to make this first phase of the project successful, particularly to Capt. Arthur L. Pavel and to Dr. Paul L. Rothwell, the Contract Monitor, who provided technical guidance throughout this phase of the program.

TABLE OF CONTENTS

List of Illustrations

List of Tables

1. INTRODUCTION

It has been found that in the presence of magnetospheric substorm particles a satellite may charge to negative potentials as high as ~10kV, and to several hundred volts while sunlit. This charge phenomenon has been reported by DeForest (Refs. 1.1 and 1.2). Since this charge buildup can have significant consequences in terms of proper satellite operation, the Air Force is instrumentating a satellite to investigate this effect. One of the instruments to be orbited on that satellite is the Rapid Scan Particle Detector, designated as SC5, which is the subject of this report.

The instrument is designed to make simultaneous measurements along two orthogonal axes of electrons with energy between 50 eV and 10 MeV and of protons in the range of 50 eV to 35 MeV. Each axis incorporates 4 electrostatic analyzers (ESA) and 2 solid state spectrometers (SSS). The 4 ESA's are arranged in 2 complementary energy ranges for electrons and protons. The low energy ESA's cover the energy range 0.05 to 1.7 keV while the high energy ESA's cover the 1.7 to 60 keV range. Four measurements are made over these ranges, plus a background measurement. The electron SSS covers the 30 to 10,000 keV range. Ten measurements are made over these ranges, in five groups of two (coincidence and ambicoincidence).

The instrument's digital output data is read every 200 ms, thus a complete energy spectrum can be generated every 1 second. A second output - pulse amplitude modulated - provides data from a high speed digital count ratemeter (~230 μs integrating time). The input to the ratemeter is selected by a multiplexer from one of the 8 ESA and 8 SSS outputs. Control logic, programmable by ground command, determines the sweep rate of the ESA or SSS and selects the output from the detectors to be processed by the ratemeter. Very high time resolution data can be generated by the latter circuit. If the sweep rate of the ESA's or SSS's is decreased, or fixed, the time resolution of portions of the spectrum

1

can be enhanced. A detailed description of the design aspect of this instrument is given in Scientific Report No. 1 (Ref. 1.3) and will not be repeated here.

As a result of the delayed selection of a Spacecraft Integrator the interface control document (ICD) only became available in final form just prior to this report date. The ICD specifies a serial entry command input rather than a parallel entry for which the instrument was originally designed. This required a redesign of the interface circuit for the command input. Also affected by the ICD was the PAM data assignment, and its subcommutated mode frame assignment, as well as the timing and control logic for this circuit.

The ESA uses a Spiraltron electron multiplier (SEM) for the detection of charged particles. Laboratory measurements were conducted with the SEM to determine 1) the relative efficiency for monoenergetic electrons and 2) the sensitivity to electrons incident on the outside of its glass body. The relative efficiency is measured for three selected electron energies, .47 keV, 7.5 keV and 15 keV. No significant variation of efficiency distribution across the funnel diameter is found for the three energies. The sensitivity to electron irradiation is measured with a Sr-Y-90 source and shows that 1/8 in. of brass covering 3/4 in. length of the Spiraltron (starting from funnel end) gives adequate shielding for ≤ 2.2 MeV electrons. A completed ESA assembly has been tested for its response to vacuum ultraviolet radiation. Under worst case conditions the UV induced accumulated counts per year compute to $\sim 1.7 \times 10^{10}$ counts, which is appreciably less than the minimum expected lifetime of the SEM, given as 2×10^{11} counts.

The electron solid state spectrometer design was slightly modified by introducing an absorber between the front and back surface barrier detectors. This was done to improve the spectral information obtained at and above 1 MeV.

The long term reliability of complementary metal oxide semiconductor (CMOS) integrated circuits has been improved by the use of radiation hardened CMOS devices throughout.

The package configuration for the Rapid Scan Particle Detector has been finalized. Compared to the original size (Ref. 1.3) the package is reduced by 2 in. in width and length, respectively. The field of view and the location of the detector entrance collimators have been defined. A mechanical interface control drawing, an analytical thermal model and an electrical interface control drawing have been completed. Housings for the ESA and SSS subassemblies have been fabricated as well as the preamplifier circuits for the ESA detectors. The design for the multiple output DC/DC converter has been completed, and fabrication of a prototype has been started. Details of the design development and construction are presented in Sections 2 and 3, respectively and conclusions are given in Section 4.

2. DESIGN DEVELOPMENTS

This instrument performs a differential energy analysis of 0.05 to 10,000 keV electrons and 0.05 to 35,000 keV protons. This is accomplished by using low energy ESA's to cover the 0.05 to 1.7 keV range, high energy ESA's to cover the 1.7 to 60 keV range, and solid state spectrometers for measurements above that range. Two complete sets of detectors are used, one of which is to be oriented perpendicular to the satellite spin axis and the other parallel to the spin axis. A simplified instrument block diagram is shown in Fig. 2.1 which reflects the redesign of the command interface as well as the deletion, addition or change of certain signals provided by the spacecraft. The spin pulse and 1 MHz clock signals previously controlling the PMA timing are deleted. The timing is now generated by an internal 1 MHz clock and the control circuitry which derives an additional 1 Hz sync. and an 8 kHz clock signal (previously 16 kHz) from the spacecraft telemetry. The command input features an added magnitude command interface, converting the serial command word into parallel entry.

The instrument package has been reduced to a volume of approximately 600 cu. in. (.35 cu. ft.) measuring 10x10x6 in., not including the
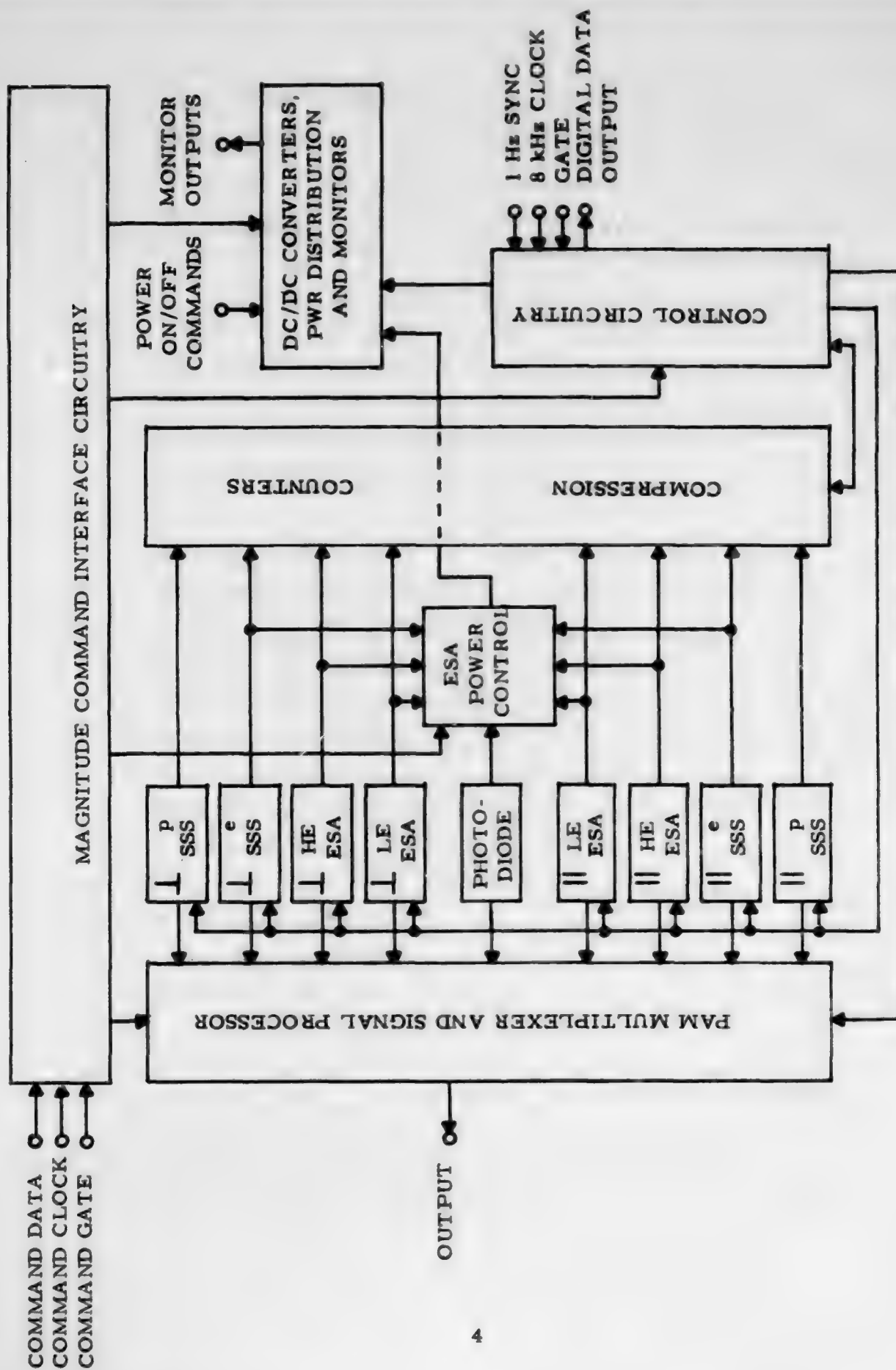
Fig. 2.1. Simplified Instrument Block Diagram.

4

small mounting tabs.　　An instrument outline drawing is shown in Fig. 2.2. The location and geometry of the detector entrance collimators have been changed slightly.　Two groups of 6 apertures are located in two opposite corners of the instrument with well defined field of views being mutually perpendicular.　Thus, one group will be oriented with a field of view parallel to, and the other perpendicular to, the spin axis.

　　　　A detailed discussion of those sub-assemblies affected by the integrator's final interface control document (IDC), or those which have been improved or tested for performance, is given in the following sections.

2.1 Electrostatic Analyzer

　　　　Three separate tests were made with a prototype ESA to determine: 1) the relative efficiency of the SEM with monoenergetic electrons, 2) the response to vacuum ultraviolet radiation and 3) the sensitivity of the SEM to electrons incident on the outside of its glass body.　Tests were also conducted to determine the absolute detection efficiency.　The relative efficiency of the funnel for monoenergetic electrons has been measured with the test setup of Fig. 2.3.　A potential of +50V is applied to the source to reduce secondary emission.　By scanning a monoenergetic electron beam across the diameter of the funnel, the relative efficiency is determined at 8 discrete positions.　Figures 2.4 and 2.5 are graphs of such scans with the funnel biased at +500V (V_F = 500V) and ground potential, respectively. The graphs show the relative response for three selected monoenergetic electron energies, namely, .47 keV, 7.5 keV, 15 keV, normalized to their value at the center.　It can be seen that no significant variation of the distribution of efficiency across the funnel diameter is found for the three energies.

　　　　The response of the SEM to solar Lyman α has been determined with a krypton lamp, EMR 582K-09, whose main output is at 1200Å. Measurements made with this UV source indicate that the SEM count rate when viewing the sun directly will be of the order of 10 kcps.　The SEM

5
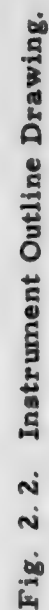
Fig. 2.2. Instrument Outline Drawing.
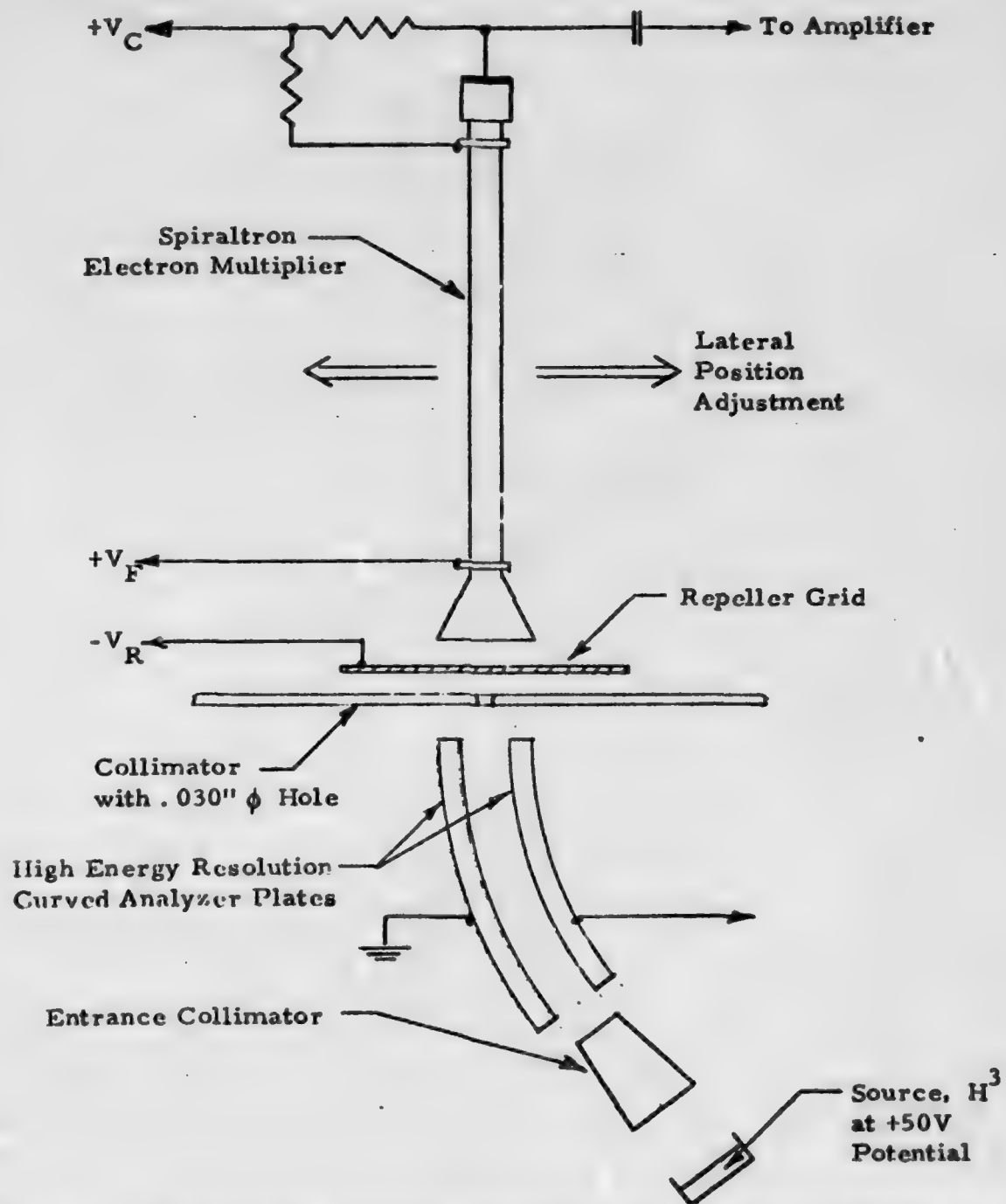
Fig. 2.3. Test Setup for Relative Efficiency Scan and Source Spectral Shape.

Fig. 2.4. Relative Efficiency Scan for Monoenergetic Electrons.

8

Fig. 2.5. Relative Efficiency Scan for Monoenergetic Electrons.

Spiraltron Relative Efficiency for Monoenergetic Electrons

Source: H^3 at +50V potential

$V_C = 3200V$, $V_F = 0V$, $V_R = -30V$

Electron Energies: 7.5 keV
15.0 keV
0.47 keV

Collimator Diameter

Active Funnel Area

Collimator Position

Normalized Relative Count Rate

1.0

.8

.6

.4

.2

0 1 2 3 4 5 6 7 8

9
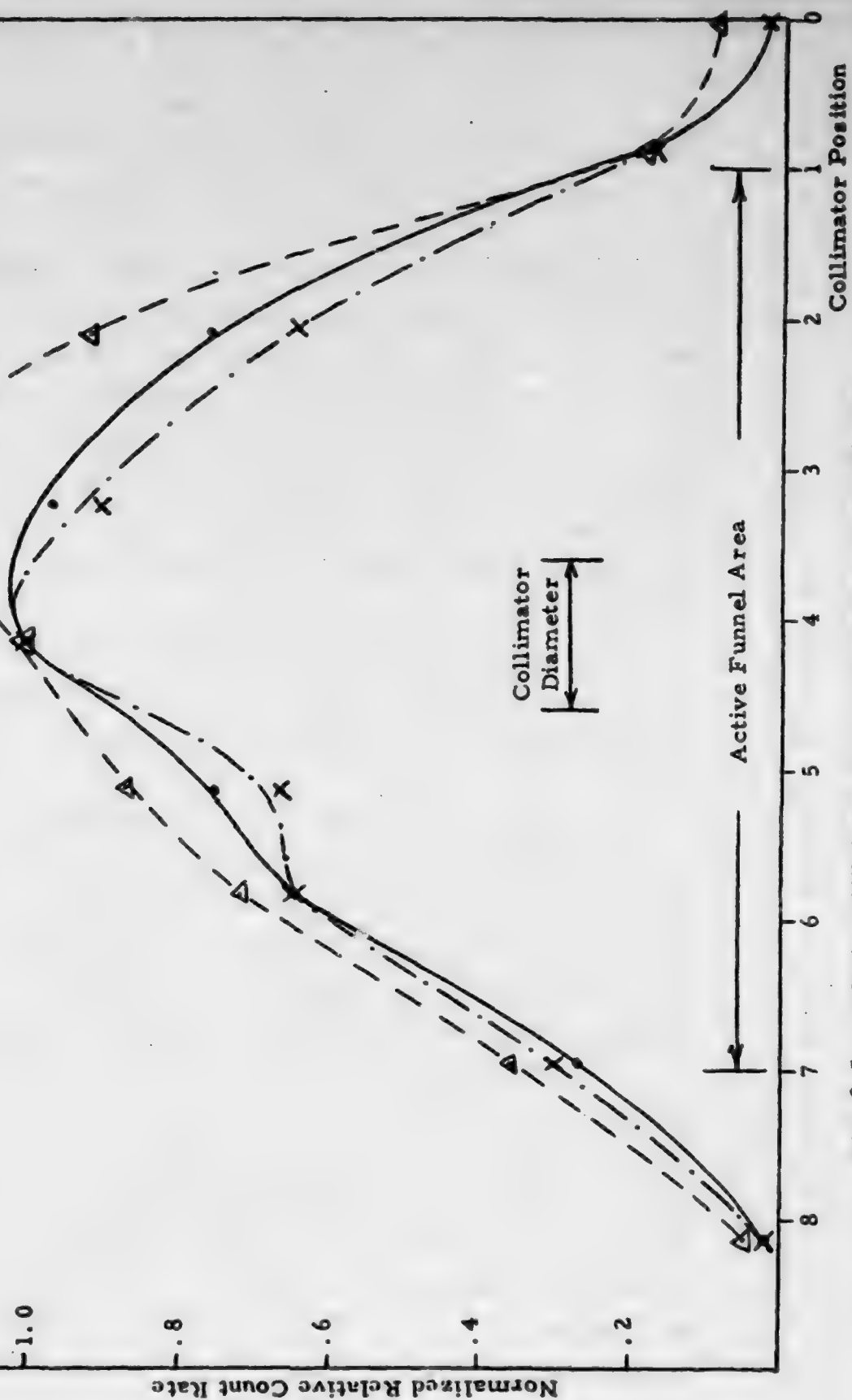
full width view angle is approximately 20° or 1/18 of a satellite rotation. Thus, under worst conditions the SEM is viewing the sun directly for 1/18 the time of expected instrument lifetime. With a UV induced count rate of 10 kcps the accumulated counts per year compute to approximately 1.7×10^{10} counts. This is appreciably less than the minimum expected lifetime of the SEM, given as 2×10^{11} counts, and turning off the ESA every time it is viewing the sun is not absolutely required. However, to increase reliability it is planned to incorporate a sun sensor (photodiode) which shuts down the ESA power for a duration equivalent to 20° roation. For added flexibility this photodiode control can be disabled by ground command. The lifetime of the SEM is further enhanced by the ground controlled increase of its bias H. V.

The above calculation of accumulated counts assumes that the instrument is on 24 hours a day for 365 days, and that the sun will be in the equatorial plane of the satellite's spin axis, neither of which is likely to be true.

The recently measured electron spectrum at synchronous orbit by Aerospace (J. B. Blake) has been incorporated in the ICD as a guide for long term reliability aspects of the on-board instruments. Based on this new penetrating electron spectrum, laboratory measurements of the Spiraltron electron multiplier (SEM) were made to determine the required amount of shielding to prevent false stimulation of output pulses by these electrons.

The Spiraltron electron multiplier (SEM) for the ESA assembly is known to produce output pulses for energetic electrons penetrating the glass envelope of the detector. Tests were conducted to verify this phenomenon and to determine the length over which the SEM would be sensitive to such radiation. A collimated Sr-Y-90 source of 2.2 MeV maximum energy was employed to irradiate the envelope over a narrow portion of its length. Scanning the full length of the Spiraltron with and without shielding around it determined the required amount and configuration of shielding. Preliminary results show that 1/8 in. of brass covering a 3/4 in. length of the

10

Spiraltron (starting from funnel end) seems to give adequate shielding for
≤2.2 MeV particles. Considering that the SEM is surrounded by various
spacecraft and experiment materials with an average equivalent thickness
of brass amounting to approximately 1/16 in., the additional required shield-
ing should be 1/16 in. of brass. The latter will be machined or formed so
as to fit closely the dimensions of the Spiraltron itself in order to minimize
added weight.

In order to determine the absolute detection efficiency it is neces-
sary to measure two quantities: 1) the relative spectral response of the H^3
source, and 2) the absolute electron flux from that source. The first of
these measurements has been carried out and the results are plotted in
Fig. 2.6. The spectrum differs somewhat from that of standard H^3, be-
cause the source is thick and has a cover. The peak is in the correct
location. The second quantity has been measured by use of a Faraday cup
under vacuum and an external digital electrometer. Preliminary results
with a tritium source (H^3) of 75 mCi nominal intensity show that the elec-
tron spectrum peaks at 7-10 keV with a flux of about 1.2×10^7 el (cm^2-sec-
sr-keV). The measurement system is presently being improved to reduce
errors from leakage currents to allow precise measurement of the spec-
tral shape.

2.2 Solid State Spectrometer

The electron solid state spectrometer has been modified by adding
an absorber between the two detectors. This improves spectral data at
high energies by giving a differential flux measurement at 1 MeV, and a
threshold measurement above 1 MeV. Revised values for ΔE, detection
energy range and detection mode for the electron solid state spectrometer
are given in Table 2.1.

Relative Spectrum of H³ Source

Source at +50V potential

--- $V_C = 3700V$, $V_F = 500V$, $V_R = -30V$

— $V_C = 3200V$, $V_F = 0V$, $V_R = -30V$

E [keV]

Normalized Relative Count Rate
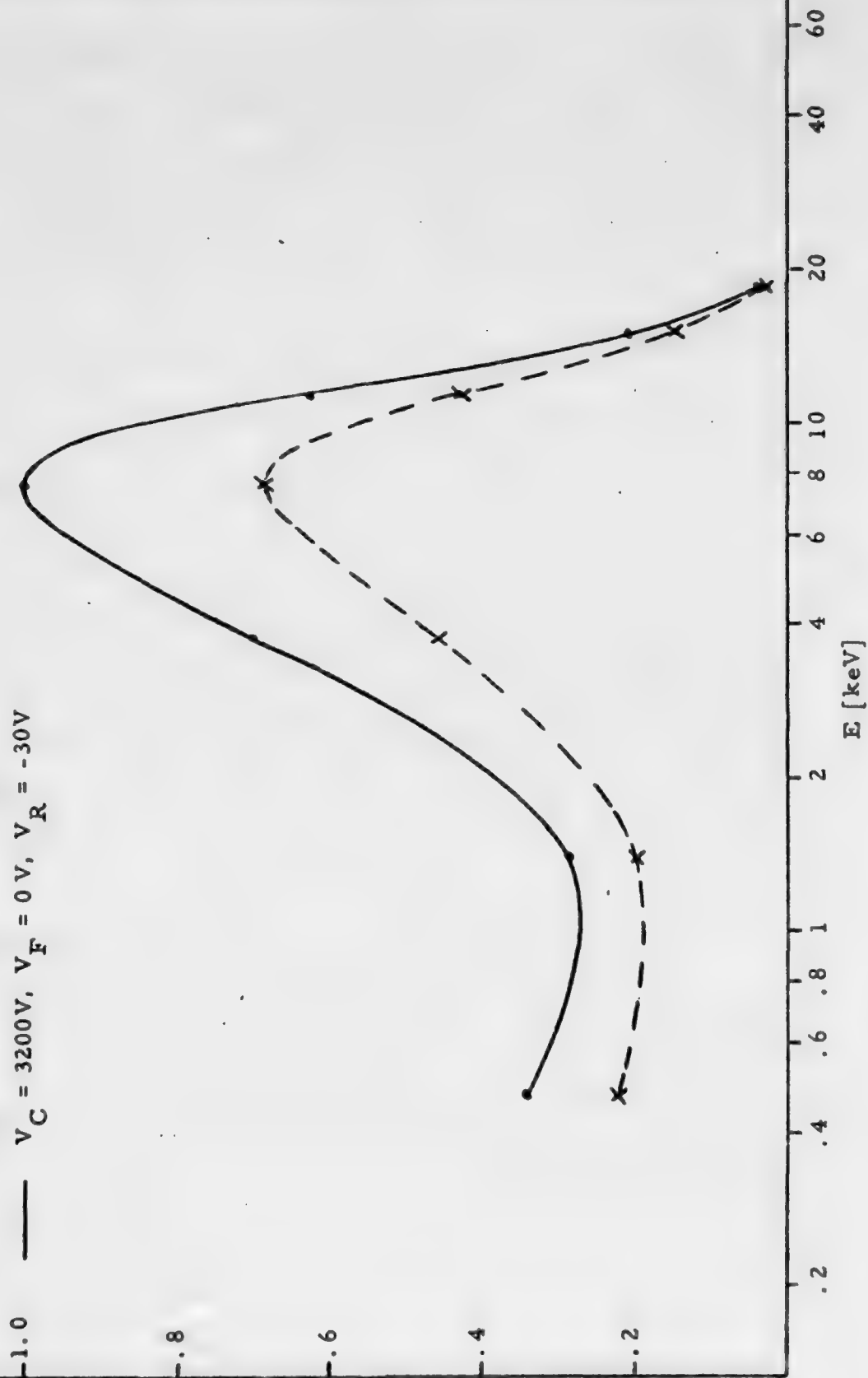
Fig. 2.6. Relative Spectral Distribution of Tritium Source.

Table 2.1

Energy Detection Ranges for the Electron Solid State Spectrometer

Channel designation	ΔE energy loss range (keV)	Electron detection energy range (keV)	Proton contaminant range (keV)	Mode type
EA0	25-41	30-45	255-270	anti
EA1	41-67	45-70	270-290	"
EA2	67-118	70-120	290-330	"
EA3	118-300	120-550	330-365	"
EA4	168-300	170-265	365-430	"
EC0	25-41	950-∞	-	coinc
EC1	41-67	980-1100	-	"
EC2	67-118	70-950	-	anti
EC3	-	950-∞	-	single
EC4	-	980-1100	-	"

2.3 Broadband Data Multiplexer and Signal Processor

A block diagram of this subsystem is shown in Fig. 2.7. The 8 pulse outputs from the ESA's, the 8 pulse outputs from the SSS's and the 2 fixed threshold pulse outputs from the e SSS's are applied to the inputs of a digital multiplexer. One of these inputs, as selected by the timing and control logic, is directed to the input of the signal processor.

The signal processor is a high time resolution digital count rate-meter, controlled by an internal 262.144 kHz clock, as shown in Fig. 2.8 - the processor timing diagram. The selected input counts are accumulated in a 5 bit compression counter (3 bit mantissa plus 2 bit exponent) while the ENABLE line is high (236.5 μsec). The counter contents are then strobed into a 5 bit latch, the counter is reset, and the next accumulation interval started. The contents of the 5 bit latch are applied to a D to A converter yielding the output voltage versus input count characteristic shown in Table 2.2. This arrangement assures the resolution of single

13

Fig. 2.7. Broadband Data Multiplexer and Signal Processor.

14

262. 144 kHz

BD CTR TRANSFER

BD CTR RESET
BD CTR ENABLE

244. 1 μ sec
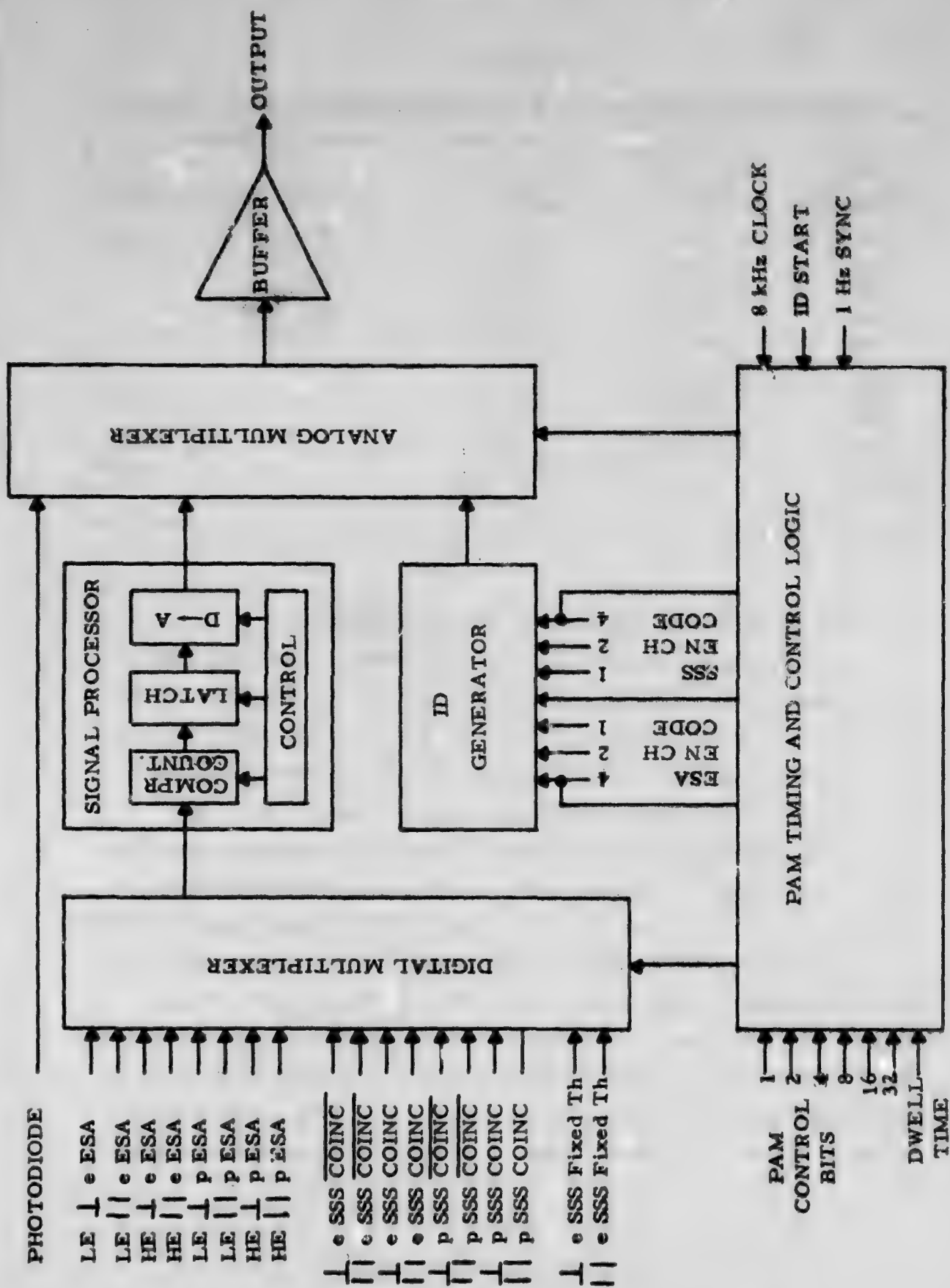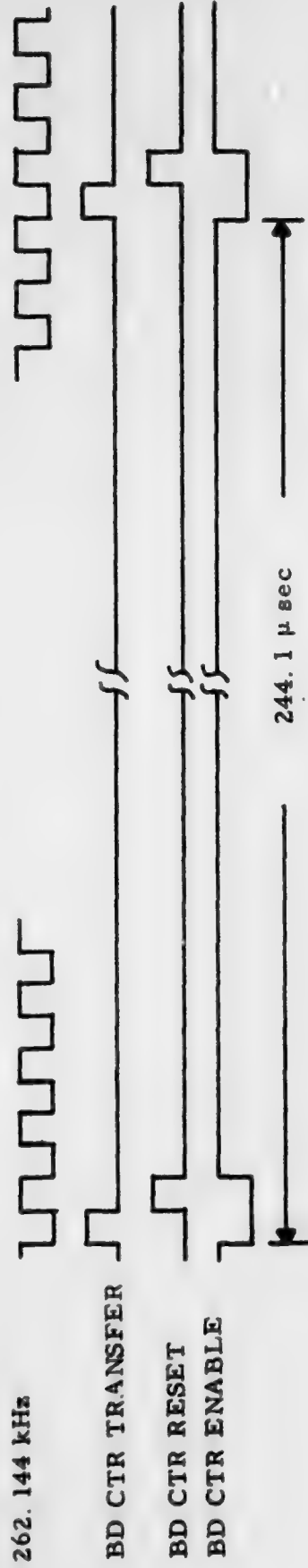
Fig. 2.8. Broadband Data Signal Processor Timing.

SIGNAL OUTPUT

H 244. 1 μ sec

ID OUTPUT

5. 0V

2. 5V

0. 0V

8 kHz CLOCK

ID START
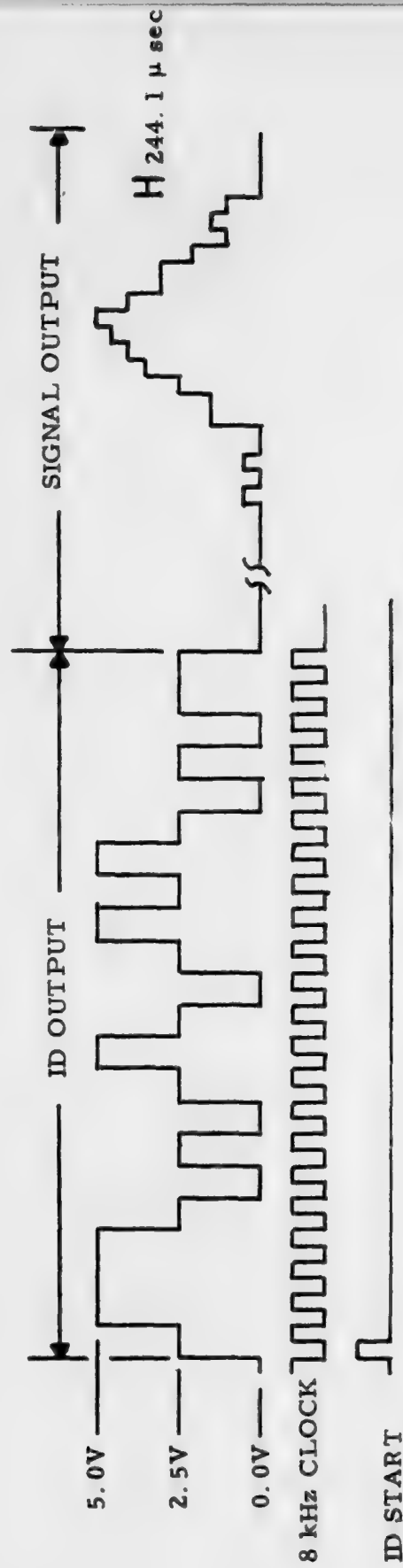
Fig. 2.9. Typical Broadband Data Output.

15

Table 2.2

Broadband Data Ouput Voltage Level
vs Input Counts (236.5 sec accumulation time)

Input Counts	Counter State		Nominal Output V
	Exponent	Montissa	
0	00	000	0.000
1	00	001	0.161
2	00	010	0.323
3	00	011	0.484
4	00	100	0.645
5	00	101	0.806
6	00	110	0.968
7	00	111	1.129
8,9	01	000	1.290
10,11	01	001	1.452
12,13	01	010	1.613
14,15	01	011	1.774
16,17	01	100	1.935
18,19	01	101	2.097
20,21	01	110	2.258
22,23	01	111	2.419
24-27	10	000	2.581
28-31	10	001	2.742
32-35	10	010	2.903
36-39	10	011	3.065
40-43	10	100	3.226
44-47	10	101	3.387
48-51	10	110	3.548
52-55	10	111	3.710
56-63	11	000	3.871
64-71	11	001	4.032
72-79	11	010	4.193
80-87	11	011	4.355
88-95	11	100	4.516
96-103	11	101	4.677
104-111	11	110	4.839
112-119	11	111	5.000

counts at low rates while still providing adequate accuracy at higher count rates. The use of a 5 bit compression counter and a 6.5 μsec accumulation time provides for satisfactory operation up to count rates of 500 kHz, which should be quite adequate in this application.

The output of the signal processor along with the UV photodiode signal and the ID generator output are fed to an analog multiplexer. One of these inputs, again selected by the timing and control logic, is fed through a unity gain buffer amplifier to the satellite PAM signal processing circuitry.

The Broadband Data channel assignment is controlled by 6 bits from the magnitude command. These 6 bits are applied to the timing and control logic allowing 64 possible assignment modes as shown in Tables 2.3 and 2.4. In the subcommutated modes the broadband data channel is assigned to each unit for a complete energy sweep, or if the unit is not sweeping, for a single digital data accumulation time (0.2 sec). The switch to the next unit is initiated as the energy channel goes from 4 to 0, or at the beginning of a digital data accumulation interval. An additional bit from the magnitude command is used to control the subcommutated modes dwell time - setting this bit changes the above dwell time to 10 energy sweeps or 70 seconds respectively.

The Broadband Data channel assignment, and the energy channel of the unit to which it is assigned, are specified by an 8 bit ID word which is generated every 200 msec - at the beginning of each data accumulation period. The ID word format is given in Table 2.5 and a typical broadband data output is shown in Fig. 2.9. Note that each ID word is preceded by a 5.0 volt synchronization level and that a pseudo RZ format is used wherein the output goes to 2.5 volts between data bits. These two levels plus a zero volt logic output level (assuming at least one ID bit is zero) give a 3 point calibration of the entire PAM processing system.

2.4 Magnitude Command Interface Circuitry

A block diagram of the magnitude command interface circuity is shown in Figure 2.10. This circuitry converts the 22 bit serial command

17

Table 2.3

Broadband Data Channel Assignments

Control Bits						Channel Assignments	
32	16	8	4	2	1		
0	0	0	0	0	0	Subcomm mode	1
0	0	0	0	0	1	Photodiode	
0	0	0	0	1	0	Subcomm mode	2
0	0	0	0	1	1		3
0	0	0	1	0	0		4
0	0	0	1	0	1		5
0	0	0	1	1	0		6
0	0	0	1	1	1		7
0	0	1	0	0	0		8
0	0	1	0	0	1		9
0	0	1	0	1	0		10
0	0	1	0	1	1		11
0	0	1	1	0	0		12
0	0	1	1	0	1		13
0	0	1	1	1	0		14
0	0	1	1	1	1		15
0	1	0	0	0	0		16
0	1	0	0	0	1	⊥ e SSS fixed threshold	
0	1	0	0	1	0	Subcomm mode	17
0	1	0	0	1	1		18
0	1	0	1	0	0		19
0	1	0	1	0	1		20
0	1	0	1	1	0		21
0	1	0	1	1	1		22
0	1	1	0	0	0		23
0	1	1	0	0	1		24
0	1	1	0	1	0		25
0	1	1	0	1	1		26
0	1	1	1	0	0		27
0	1	1	1	0	1		28
0	1	1	1	1	0		29
0	1	1	1	1	1		30
1	0	0	0	0	0		31
1	0	0	0	0	1		32
1	0	0	0	1	0	‖ e SSS fixed threshold	
1	0	0	0	1	1	Subcomm mode	33
1	0	0	1	0	0		34
1	0	0	1	0	1		35
1	0	0	1	1	0		36

18

Table 2. 3 (cont'd)

1	0	0	1	1	1						37
1	0	1	0	0	0						38
1	0	1	0	0	1						39
1	0	1	0	1	0						40
1	0	1	0	1	1						41
1	0	1	1	0	0						42
1	0	1	1	0	1						43
1	0	1	1	1	0						44
1	0	1	1	1	1						45
1	1	0	0	0	0	LE	⊥	e	ESA		
1	1	0	0	0	1	LE	||	e	ESA		
1	1	0	0	1.	0	HE	⊥	e	ESA		
1	1	0	0	1	1	HE	||	e	ESA		
1	1	0	1	0	0	LE	⊥	p	ESA		
1	1	0	1	0	1	LE	||	p	ESA		
1	1	0	1	1	0	HE	⊥	p	ESA		
1	1	0	1	1	1	HE	||	p	ESA		
1	1	1	0	0	0		⊥	e	SSS	c̄	
1	1	1	0	0	1		||	e	SSS	c̄	
1	1	1	0	1	0		⊥	e	SSS	c	
1	1	1	0	1	1		||	e	SSS	c	
1	1	1	1	0	0		⊥	p	SSS	c̄	
1	1	1	1	0	1		||	p	SSS	c̆	
1	1	1	1	1	0		⊥	p	SSS	c	
1	1	1	1	1	1		||	p	SSS	c	

Table 2.4

Broadband Data Subcommutated Mode Frame Assignment

Table 2.4A
(Subcomm Mode 1)

Subcomm Mode	Frame#							
	1	2	3	4	5	6	7	8
1	LE⊥e ESA	LE‖e ESA	HE⊥e ESA	HE‖e ESA	LE⊥p ESA	LE‖p ESA	HE⊥p ESA	HE‖p ESA

Subcomm Mode	Frame#							
	1	2	3	4	5	6	7	8
1	⊥e SSS c̄	‖e SSS c̄	⊥e SSS c	‖e SSS c	⊥p SSS c̄	‖p SSS c̄	⊥p SSS c	‖p SSS c

20

Table 2.4B

(Subcomm modes 2-23)

Subcomm Mode	Frame # 1	2	3	4	5	6	7	8
2	LE ⊥ e ESA	HE ⊥ e ESA	LE ⊥ p ESA	HE ⊥ p ESA	⊥ e SSS c̄	⊥ e SSS c	⊥ p SSS c̄	⊥ p SSS c
3	LE ‖ e ESA	HE ‖ e ESA	LE ‖ p ESA	HE ‖ p ESA	‖ e SSS c̄	‖ e SSS c	‖ p SSS c̄	‖ p SSS c
4	LE ⊥ e ESA	LE ‖ e ESA	HE ⊥ e ESA	HE ‖ e ESA	⊥ e SSS c̄	‖ e SSS c	⊥ e SSS c	‖ e SSS c
5	LE ⊥ p ESA	LE ‖ p ESA	HE ⊥ p ESA	HE ‖ p ESA	⊥ p SSS c̄	‖ p SSS c	⊥ p SSS c	‖ p SSS c
6	LE ⊥ e ESA	LE ‖ e ESA	LE ⊥ p ESA	LE ‖ p ESA	⊥ e SSS c̄	‖ e SSS c	⊥ p SSS c̄	⊥ p SSS c̄
7	HE ⊥ e ESA	HE ‖ e ESA	HE ⊥ p ESA	HE ‖ p ESA	⊥ e SSS c	‖ e SSS c	⊥ p SSS c	‖ p SSS c
8	LE ⊥ e ESA	HE ⊥ e ESA	⊥ e SSS c̄	⊥ e SSS c				
9	LE ‖ e ESA	HE ‖ e ESA	‖ e SSS c̄	‖ e SSS c				
10	LE ⊥ p ESA	HE ⊥ p ESA	⊥ p SSS c̄	⊥ p SSS c				
11	LE ‖ p ESA	HE ‖ p ESA	‖ p SSS c̄	‖ p SSS c				
12	LE ‖ e ESA	LE ‖ e ESA	⊥ e SSS c̄	⊥ p SSS c				
13	LE ‖ e ESA	LE ‖ p ESA	‖ e SSS c̄	‖ p SSS c				
14	HE ⊥ p ESA	HE ⊥ p ESA	⊥ e SSS c	⊥ p SSS c				
15	HE ‖ p ESA	HE ‖ p ESA	‖ e SSS c	‖ p SSS c				
16	LE ⊥ e ESA	LE ‖ e ESA	HE ⊥ e ESA	HE ‖ e ESA	LE ⊥ p ESA	LE ‖ p ESA	HE ⊥ p ESA	HE ‖ p ESA
17	LE ⊥ e ESA	HE ⊥ e ESA	LE ⊥ p ESA	HE ⊥ p ESA				
18	LE ‖ e ESA	HE ‖ e ESA	LE ‖ p ESA	HE ‖ p ESA				
19	LE ⊥ e ESA	LE ‖ e ESA	HE ⊥ e ESA	HE ‖ e ESA				
20	LE ⊥ p ESA	LE ‖ p ESA	HE ⊥ p ESA	HE ‖ p ESA				
21	LE ⊥ e ESA	LE ‖ e ESA	LE ⊥ p ESA	LE ‖ p ESA				
22	HE ⊥ e ESA	HE ‖ e ESA	HE ⊥ p ESA	HE ‖ p ESA				
23	LE ⊥ e ESA	HE ⊥ e ESA						

21

Table 2.4C

(Subcomm modes 24-45)

Subcomm Mode	Frame #							
	1	2	3	4	5	6	7	8
24	LE ‖ e ESA	HE ‖ e ESA						
25	LE ⊤ p ESA	HE ⊥ p ESA						
26	LE ‖ p ESA	HE ‖ p ESA						
27	LE ⊥ e ESA	LE ⊥ p ESA						
28	LE ‖ e ESA	LE ‖ p ESA						
29	HE ⊤ p ESA	HE ⊥ p ESA						
30	HE ‖ p ESA	HE ⊤ p ESA						
31	‖ e SSS c̄	‖ e SSS c̄	⊤ e SSS c	‖ e SSS c	⊤ p SSS c	⊥ p SSS c̄	⊤ p SSS c	⊤ p SSS c
32	⊤ e SSS c̄	⊤ e SSS c	⊤ p SSS c̄	‖ p SSS c				
33	‖ e SSS c̄	‖ e SSS c	‖ p SSS c̄	⊥ p SSS c				
34	⊤ e SSS c̄	‖ e SSS c̄	⊤ e SSS c	⊥ e SSS c				
35	⊤ p SSS c	‖ p SSS c̄	⊤ p SSS c	⊤ p SSS c				
36	⊤ e SSS c̄	‖ e SSS c̄	⊤ p SSS c̄	‖ p SSS c̄				
37	⊤ e SSS c	⊤ e SSS c	⊤ p SSS c	‖ p SSS c				
38	⊤ e SSS c̄	⊤ e SSS c						
39	‖ e SSS c	‖ e SSS c						
40	⊤ p SSS c̄	⊤ p SSS c						
41	⊤ p SSS c̄	‖ p SSS c						
42	⊤ e SSS c̄	‖ p SSS c						
43	⊤ e SSS c̄	⊤ p SSS c						
44	‖ e SSS c	⊤ p SSS c						
45	‖ e SSS c	‖ p SSS c						

22

Table 2.5
Broadband Data ID Word Format

| PAM Assignment				Group ID		Unit ID			Energy Channel		
				1	2	3	4	5	6	7	8
LE ⊥ e ESA				0	0	0	0	0	ESA EN CH 4	ESA EN CH 2	ESA EN CH 1
LE ‖ e ESA				0	0	0	0	1			
HE ⊥ e ESA				0	0	0	1	0			
HE ‖ e ESA				0	0	0	1	1			
LE ⊥ p ESA				0	0	1	0	0			
LE ‖ p ESA				0	0	1	0	1			
HE ⊥ p ESA				0	0	1	1	0			
HE ‖ p ESA				0	0	1	1	1			
⊥ e SSS $\overline{COINC}$				0	1	0	0	0	SSS EN CH 4	SSS EN CH 2	SSS EN CH 1
‖ e SSS $\overline{COINC}$				0	1	0	0	1			
⊥ e SSS COINC				0	1	0	1	0			
‖ e SSS COINC				0	1	0	1	1			
⊥ p SSS $\overline{COINC}$				0	1	1	0	0			
‖ p SSS $\overline{COINC}$				0	1	1	0	1			
⊥ p SSS COINC				0	1	1	1	0			
‖ p SSS COINC				0	1	1	1	1			
⊥ e SSS Fixed Th				1	0	0	0	0	x	x	x
‖ e SSS Fixed Th				1	1	0	0	0	x	x	x
Photodiode				1	x	1	1	1	x	x	x

23
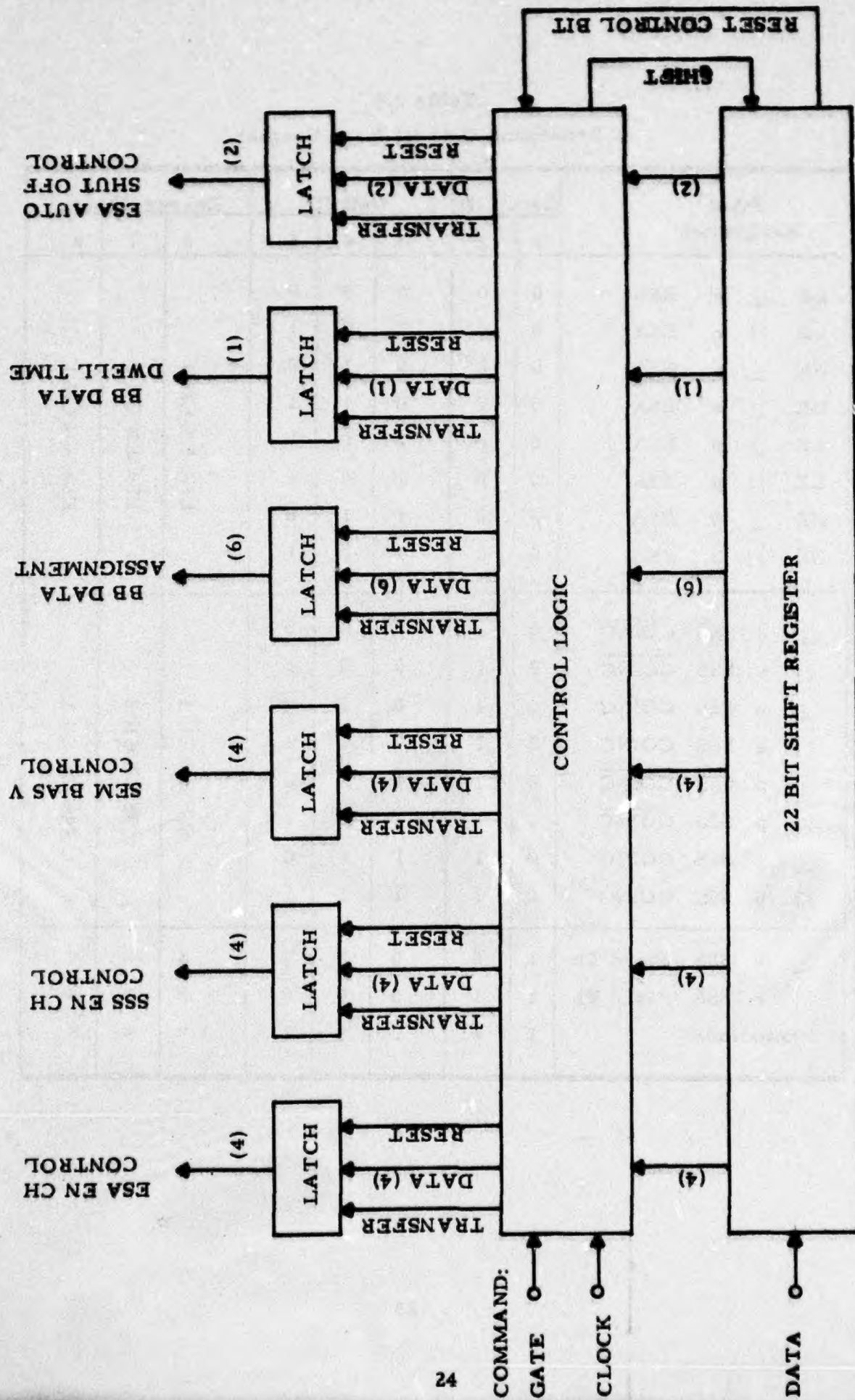
Fig. 2.10. Magnitude Command Interface Circuitry Block Diagram.

24

received from the spacecraft into the parallel format required by the various instrument subsystems. The 22 bits are utilized as follows:

        4 bits - ESA energy channel control
        4 bits - SSS energy channel control
        4 bits - SEM bias voltage control
        6 bits - Broadband data channel assignment
        1 bit - Broadband data subcomm dwell time
        2 bits - ESA auto shutoff circuitry control
       ___
        21

The remaining bit is used as a reset control bit. The control logic is such that a latch:

        1) is updated if any of its data bits are set and the reset bit is not set

        2) is cleared if any of its data bits are set and the reset bit is set

        3) remains unchanged if all of its data bits are zero.

This scheme allows completely independent control of the various logical bit groups - the ESA energy channel control bits may be changed without affecting the SSS energy channel control bits, or any of the other control bits. This scheme also allows for simultaneous updating of 2 or more groups of control bits - the SSS and ESA energy channel control bits may be changed with a single magnitude command.

2.5 System Parameters

        Since the outline dimensions of all major system components are now well specified, the package configuration and systems wiring of the Rapid Scan Spectrometer have been finalized. This made it possible to characterize the system and submit the following documentation to the integrator:

        1) The mechanical interface control drawing showing mounting arrangement, center of gravity and the mass moment of inertia. (D4061)

        2) An analytical thermal model of the system, based on power dissipation of major components, their location and the structural materials used. (D4073)

3) The electrical interface control drawing showing all input and and output connections, pin assignments and connector type. Typical output circuits are given with output voltage range and impedance. (D4093)

3. FABRICATION

Eight housings for the electrostatic analyzer subassemblies for two satellite systems have been completed. Four housings for the solid state spectrometer have been completed. Since the housings for the electron and proton spectrometer are identical, they can be used to complement two rapid scan spectrometers with electron detectors in case it is decided that no proton detectors are to be flown. If the proton detectors are to be included, four more housings will have to be constructed. Eight preamplifier boards for the electrostatic analyzer have been assembled and functionally tested.

4. CONCLUSIONS

The design of the Rapid Scan Spectrometer has been completed.

The development work reported herein shows that considerable redesign had to be done to accomodate the serial entry command input required by the integrator. Further, the command word was increased to 22 bits (16 previously) allowing for the monitoring of 64 assignment modes (16 previously) of the broadband multiplexer, thus increasing the versatility of the instrument. Of course, the additional command bits also increased the complexity of the control logic for the broadband multiplexer. The ESA tests served to enhance the reliable operation of this unit under conditions of undesirable UV and electron irradiation. The relative efficiency measurements will ultimately be used to arrive at an absolute calibration of the SEM electron detection efficiency. A very worthwhile improvement of the electron spectrum information available from the SSS's has been achieved with the simple addition of an absorber between the front and back detectors of that unit.

The fabrication of subassemblies has progressed at a normal rate indicating that the delivery schedule can be met.

26

References

1.1   DeForest, S. E., J. Geo. Resch. <u>77</u>, 651-659 (1972).

1.2   DeForest, S. E. and McIlwain, C. E., J. Geo. Resch. <u>76</u>, 3587-3611 (1971).

1.3   Jean L. Hunerwadel, Paul R. Morel, Frederick A. Hanser and Bach Sellers, Design of Instrumentation Suitable for the Investigation of Charge Buildup Phenomena at Synchronous Orbit, report AFCRL-TR-75-0365, July 1975. Scientific Report No. 1 for Contract No. F19628-74-C-0217.